Journal of Computational Physics 230 (2011) 7384–7399

Contents lists available at ScienceDirect

Journal of Computational Physics

journal homepage: www.elsevier.com/locate/jcp

Optimal constant shape parameter for multiquadric based RBF-FD method

Victor Bayona, Miguel Moscoso, Manuel Kindelan *

Gregorio Millán Institute, Universidad Carlos III de Madrid, Avenida de la Universidad 30, 28911 Leganés, Spain

ARTICLE INFO

Article history:
Received 22 December 2010
Received in revised form 3 June 2011
Accepted 5 June 2011
Available online 23 June 2011

Keywords:
Radial basis functions
Multiquadric
Mesh-free
Shape parameter

ABSTRACT

Radial basis functions (RBFs) have become a popular method for interpolation and solution of partial differential equations (PDEs). Many types of RBFs used in these problems contain a shape parameter, and there is much experimental evidence showing that accuracy strongly depends on the value of this shape parameter. In this paper, we focus on PDE problems solved with a multiquadric based RBF finite difference (RBF-FD) method. We propose an efficient algorithm to compute the optimal value of the shape parameter that minimizes the approximation error. The algorithm is based on analytical approximations to the local RBF-FD error derived in [1]. We show through several examples in 1D and 2D, both with structured and unstructured nodes, that very accurate solutions (compared to finite differences) can be achieved using the optimal value of the constant shape parameter.

1. Introduction

Radial basis functions (RBFs) were first used as an efficient technique for interpolation of multidimensional scattered data (see [11] and references therein). Later, it became popular as a truly mesh-free method for the solution of partial differential equations (PDEs) on irregular domains. This application of RBFs was first proposed by Kansa [23,24] and it is based on collocation in a set of scattered nodes.

To overcome some of the drawbacks of the global RBF method, a local RBF method was independently proposed by several authors which gave the method different names; Shu et al. [37] local multiquadric-based differential quadrature (LMQDQ) method, Tolstykh and Shirobokov [39] RBF in a "finite difference mode", Wright [42] RBF finite difference method. The method is based on approximating the solution as a linear combination of a set of identical RBFs translated to a set of (scattered) RBF centers. However, the approximation is local, so it is carried out within a small influence domain instead of a global one. As a consequence, the resulting linear system is sparse, overcoming the ill-conditioning often associated to the global method, at the cost of losing its spectral accuracy. As a result, the local RBF method approximates a differential operator at a given node as a weighted sum of the values of the sought function at some surrounding nodes. Thus, it can be considered as a generalization of the classical FD method. While in the global method the unknowns are the coordinates of the solution in the functional space spanned by the RBFs, in the local method the unknowns are the values of the solution at the scattered nodes, just the same as with the FD method. However, in the FD method the weights are computed using polynomial interpolation, and in the local RBF one they are computed by fitting an RBF interpolant through a grid point and a small number of its nearest neighbors. Since both, FD and local RBF formulas are identical in form, we will refer to the local RBF method as the RBF finite difference (RBF-FD) method, as in [42]. In the last years the RBF-FD method has been successfully applied to a great variety of problems [3,6,7,18,29,31–33,36,38,40].

Most of the RBFs used to approximate the solution to a PDE contain a shape parameter (that we denote c) that has to be chosen a priori. There is much experimental evidence showing that the accuracy of the approximated solution strongly

* Corresponding author. Fax: +34 91 624 91 29.
E-mail addresses: vbayona@ing.uc3m.es (V. Bayona), moscoso@math.uc3m.es (M. Moscoso), kinde@ing.uc3m.es (M. Kindelan).

0021-9991/$ - see front matter © 2011 Elsevier Inc. All rights reserved.
doi:10.1016/j.jcp.2011.06.005

depends on the value of this shape parameter c. For the global RBF method accuracy increases with c, but if c is too large the condition number of the resulting linear system also increases giving rise to numerical instabilities and loss of precision. Thus, the problem of how to select appropriate values for the shape parameter has been of primary concern both from the theoretical and the application points of view. As a result, a significant amount of interesting work has been carried out to address this issue for interpolation and PDE problems (either with the global or the local RBF methods). Some of the proposed techniques address the problem of how to select a single (constant) value of the shape parameter, while others address the problem of selecting different shape parameters values for each node.

For interpolation problems, Hardy [21] suggested the use of $c = 0.815d$, where d is the average distance to the nearest neighbor ($d = h$ for equispaced nodes). On the other hand, Franke [19] recommended $c = 1.25D/\sqrt{N}$, where D is the diameter of the smallest circle containing all data points ($c = 1.25\sqrt{2}h$ for equispaced nodes). A different approach was taken by Carlson and Foley [4], who pointed out that the optimal value of c was strongly dependent on the interpolated function and essentially independent on the number and location of the interpolation nodes. They also presented an algorithm that yields an effective value of c. Rippa [30] proposed a *leave-one-out* algorithm to estimate the interpolation error and use it to compute an optimal value of the shape parameter. Larsson and Fornberg [28] used the method proposed in [16] to circumvent ill-conditioning and, thereby, were able to solve interpolation problems for very large values of c. They found that, very often, the error reaches a minimum for a finite value of c. The value of the optimal shape parameter was studied and explained through approximate expansions of the interpolation error.

Regarding spatially varying shape parameters, Kansa and Carlson [25] showed through numerical experiments that using a node dependent value of c gives better accuracy than a single (constant) one. The optimal value of c was determined by numerically minimizing the root mean square error.

For the solution of PDEs with the global RBF method, it has often been argued [22,27,28] that one should push the value of the shape parameter as far as possible in order to achieve more and more accurate solutions. Accuracy should only be limited by ill-conditioning of the resulting matrix. Thus, a significant amount of work has been devoted to improve the condition number of the linear system associated to the PDE by pre-conditioning or by other techniques. This counterintuitive statement that, without roundoff error, infinite accurate solutions can be obtained with a coarse grid, was refuted by Huang et al. [22]. These authors used arbitrary precision computations to experimentally derive a formula for the error dependence on the shape parameter c and the nodal spacing h. From this formula they obtain the optimal value of the shape parameter that minimizes the error; $c = -\log\lambda/(3ah)$, where a and λ are constants that depend on the problem. Thus, for a given grid there is a maximum accuracy that can be obtained when the optimal shape parameter is used. A different approach was used by Fasshauer et al. [12–14]. They generalized Rippa's *leave-one-out* interpolation algorithm [30] to the solution of PDEs with the RBF global method.

There are also several authors that have explored the benefits of using spatially varying shape parameters with the global RBF method. Kansa and Hon [26] were first to suggest that a variable shape parameter should be related to the local curvature of the solution, and proposed an experimentally based formula to compute its value. Driscoll and Heryudono [10] proposed an adaptive algorithm based on computing residuals on a finer grid and using this information to remove or add nodes. The shape parameters were also adaptively varied by taking them proportional to the local internode distance. Wertz et al. [41] used numerical experiments to show that the shape parameter should be significantly higher at boundary nodes than at interior nodes. They also showed that introducing oscillations in the values of the shape parameters improves accuracy. Fornberg and Zuev [17] showed that the Runge phenomenon plays a major role in the error of RBF interpolation and, as a result, that it is advantageous to let the shape parameter vary spatially. They used global optimization of a certain functional to explore the benefits of node dependent values of c and confirmed the empirical observations reported in [41]. Finally, Flyer and Letho [15] used local node refinement for the solution of vortex roll-up and transport on a sphere. They used a node dependent shape parameter that varies according to the inverse of the Euclidean distance to the nearest node. However, the differentiation matrices had to be recalculated every few time steps which implied a rather high computational cost. Thus, the authors state at the conclusions section that they were exploring faster methods to calculate differentiation matrices such as localized RBF stencils.

With regards to the solution of PDEs using the local RBF method, it has been shown that, in the limit of increasingly flat basis functions ($c \to \infty$), the RBF interpolants converge to polynomial interpolants [9] and, therefore, all classical finite difference formulas can be recovered from RBF-FD formulas in the limit $c \to \infty$. There is also considerable experimental evidence [5,43] that very often there is a range of values of the shape parameter for which errors are significantly lower than errors resulting from standard finite differences.

In this paper we address the problem of how to select a single value of the shape parameter c in order to minimize the error of the approximation to a solution of a PDE with the local RBF-FD method. We show that the accuracy of the solution can be improved one or two orders of magnitude with respect to finite differences if one selects the right value of the shape parameter, and we describe an efficient technique to compute it. The technique is based on the analytical approximations to the local error derived in [1] for 1D and 2D differential operators (for structured and non-structured nodes). In this work, we use multiquadrics as RBFs since the formulas in [1] were derived for these functions. However, the technique is readily applicable to any other RBF containing a free shape parameter (Gaussians, inverse multiquadrics, ...).

In a second paper [2] we describe how to compute a spatially varying optimal shape parameter which can give rise to further significant improvements in accuracy, provided that there exists an optimal c for most of the grid points of the domain. However, if there are some nodes for which an optimal value of c does not exist, the accuracy is similar to that obtained

with the optimal constant c. For those cases, we show that using generalized multiquadrics with proper parameters guarantees the existence of an optimal c for all the nodes, and thus, very significant improvements in accuracy are obtained. However, it should be pointed out, that the constant shape parameter method described in this paper is much easier to program than the variable shape parameter one, so that the gains in accuracy might not compensate the burden of programming the variable case.

The rest of the paper is organized as follows. In Section 2, we briefly describe the local RBF-FD method, and how to compute the optimal shape parameter. In Section 3, we describe in detail the resulting numerical algorithm. Section 4 includes several examples in 1D and 2D using both structured and unstructured nodes. Finally, in Section 5 we summarize the main results of this work.

2. RBF-FD method formulation

Consider the Dirichlet problem in a bounded domain $\Omega \subset \mathbb{R}^d$

$$\begin{cases} \mathcal{L}[u(\mathbf{x})] = f(\mathbf{x}), & \text{in } \Omega, \\ u(\mathbf{x}) = g(\mathbf{x}), & \text{on } \partial\Omega, \end{cases} \tag{1}$$

where $\mathcal{L}[\cdot]$ is a differential operator and f and g are real functions. In the RBF-FD method we approximate the operator $\mathcal{L}[\cdot]$ at a node $\mathbf{x} = \mathbf{x}_j$ by a linear combination of the values of the unknown function u at n scattered nodes surrounding $\mathbf{x}_j$, which constitute its stencil. Thus,

$$\mathcal{L}[u(\mathbf{x}_j)] \approx \sum_{i=1}^{n} \alpha_{ji} u(\mathbf{x}_i), \tag{2}$$

where α_{ji} are the weighting coefficients. In the standard FD formulation, these coefficients are computed using polynomial interpolation. In the RBF-FD formulation, they are computed using interpolation with radial basis functions, thus

$$u(\mathbf{x}) = \sum_{i=1}^{n} \lambda_i \phi(r_i(\mathbf{x}), c_i), \tag{3}$$

where $r_i(\mathbf{x}) = \|\mathbf{x} - \mathbf{x}_i\|$ is the distance to the RBF center, $\|\cdot\|$ is the Euclidean norm, and $\phi(r_i(\mathbf{x}), c_i)$ is some radial function which depends on a free shape parameter c_i. In the following, we will use Hardy's multiquadric as RBF [21] with a single (constant) value of the shape parameter ($c_i = c$), thus

$$\phi(r_i(\mathbf{x}), c) = \sqrt{c^2 + r_i(\mathbf{x})^2}. \tag{4}$$

As we emphasized before, accuracy is highly dependent on the value of the shape parameter c.

Substituting (3) into (2) we can determine the unknown weighting coefficients α_{ji} by solving the system of linear equations

$$\mathcal{L}\big[\phi(r_k(\mathbf{x}_j), c)\big] = \sum_{i=1}^{n} \alpha_{ji} \phi(r_k(\mathbf{x}_i), c), \quad k = 1, \ldots, n. \tag{5}$$

Thus, the coefficients α_{ji} depend on the distances from $\mathbf{x}_j$ to the other nodes in the stencil, and on the shape parameter c. In the following, we will assume that the set of interpolation nodes with the corresponding stencils are given. Therefore, the coefficients α_{ji} will be functions of the shape parameter c only.

Consider that the domain Ω is discretized using N scattered nodes (N_I interior nodes and $N - N_I$ boundary nodes). Using (2), Eq. (1) at an interior node $\mathbf{x}_j$ can be written as

$$\sum_{i=1}^{n} \alpha_{ji}(c) u(\mathbf{x}_i) = f(\mathbf{x}_j) + \epsilon_n(\mathbf{x}_j; c), \quad 1 \leqslant j \leqslant N_I, \tag{6}$$

where $\epsilon_n(\mathbf{x}_j; c)$ is the local RBF-FD error resulting from approximating the differential operator $\mathcal{L}[.]$ with the n node RBF-FD formula (2). In matrix form, these equations can be written as

$$A(c)\mathbf{u} = \mathbf{f} + \boldsymbol{\epsilon}(c), \tag{7}$$

where $\mathbf{u}$ is the vector of exact solutions at the interior nodes, $A(c)$ is a $N_I \times N_I$ sparse matrix whose entries are the weighting coefficients $\alpha_{ji}(c)$, and $\boldsymbol{\epsilon}(c)$ is a vector formed by the local RBF-FD approximation errors $\epsilon_n(\mathbf{x}_j; c)$ at the interior nodes.

The RBF-FD approximation $\hat{\mathbf{u}}$ to the exact solution $\mathbf{u}$ is obtained by solving the discretized linear system

$$\hat{\mathbf{u}}(c) = A^{-1}(c)\mathbf{f}, \tag{8}$$

so the RBF-FD error is given by

$$\mathbf{E}(c) \equiv \mathbf{u} - \hat{\mathbf{u}}(c). \tag{9}$$

Therefore, we can state our problem as the problem of finding the value of the shape parameter c which minimizes (9) in a certain norm. We define the optimal shape parameter as the value c^* such that

$$\|\mathbf{E}(c^*)\|_\infty = \min_c \|\mathbf{E}(c)\|_\infty \equiv \min_c \|\mathbf{u} - \hat{\mathbf{u}}(c)\|_\infty. \tag{10}$$

It is apparent that in real problems the value c^* cannot be computed directly from (10) because the exact solution is not known. However, from (7) and (8) we can write

$$\|\mathbf{E}(c^*)\|_\infty = \min_c \|A^{-1}(c)\boldsymbol{\epsilon}(c)\|_\infty, \tag{11}$$

and estimate the value c^* using the analytical approximations to the local error $\boldsymbol{\epsilon}(c)$ derived in [1]. These formulas are written as series expansions in powers of h (the inter nodal distance), which are valid for $c \gg h$. The coefficients of these formulas depend on c, h, and on the value of the exact solution and its derivatives. However, as we will show later, these coefficients can be easily computed without losing accuracy using an approximate finite difference solution $\tilde{\mathbf{u}}$ instead of the exact solution $\mathbf{u}$. Using these formulas we seek for an approximate value c_e^* to the optimal shape parameter c^* such that

$$\|\mathbf{E}_e(c_e^*)\|_\infty = \min_c \|A^{-1}(c)\boldsymbol{\epsilon}_e(c)\|_\infty, \tag{12}$$

where $\boldsymbol{\epsilon}_e(c)$ is the estimated local error computed with the analytical approximations to the local error derived in [1].

3. Numerical algorithm

For a given problem (1) and a given set of N scattered nodes, the numerical method described in the previous section is implemented in the following numerical algorithm:

(1) For each interior node $\mathbf{x}_j$ determine a stencil of n surrounding nodes.
(2) Use finite differences to compute an approximate solution $\tilde{\mathbf{u}}(\mathbf{x}_j)$.
(3) Find the value c_e^* which minimizes $\|A^{-1}(c)\boldsymbol{\epsilon}_e(c)\|_\infty$. At each iteration:
   - Use (5) to compute numerically the RBF-FD coefficients $\alpha_{ji}(c)$, and therefore matrix $A(c)$.
   - Use the finite difference solution $\tilde{\mathbf{u}}(\mathbf{x}_j)$ computed in step 2 and the analytical formulas derived in [1] to estimate the local approximation error $\epsilon_n(\mathbf{x}_j; c)$ at each node, and therefore $\boldsymbol{\epsilon}_e(c) = [\epsilon_e(\mathbf{x}_1; c), \epsilon_e(\mathbf{x}_2; c), \ldots, \epsilon_e(\mathbf{x}_N; c)]^T$.
(4) Compute the optimal RBF-FD approximate solution $\hat{\mathbf{u}}(c_e^*) = A^{-1}(c_e^*)\mathbf{f}$.

In step 3 we have used matlab command `fminsearch` which finds the minimum of a non-linear function using the Nelder–Mead Simplex method.

From the point of view of computational cost, the algorithm requires the solution of two $N_I \times N_I$ sparse linear systems (steps 2 and 4), and the solution of N_I dense systems of $n \times n$ unknowns at each iteration of step 3. The typical number of iterations required is 15.

A possibility to try to improve the accuracy of c_e^* is to use an iterative procedure: once an approximate value of c_e^* is computed in step (4) and therefore a better approximation $\hat{\mathbf{u}}(c_e^*)$ to the exact solution, go back to step (3) to compute a refined value of c_e^*.

4. Example problems

In this section we will apply the numerical algorithm just described to the solution of some example problems in 1D and 2D, using both structured and non-structured nodes. We will also apply the technique to several problems that have been solved in the past with the RBF-FD method. We will show that using the optimal (constant) value of the shape parameter leads to significant improvements in accuracy.

4.1. One dimensional boundary value problem

Consider the following problem

$$\begin{cases} u_{xx} = f(x), & 0 < x < 1, \\ u(0) = 1, \quad u(1) = 1 + \frac{\sqrt{2}}{2}, \end{cases} \tag{13}$$

where $f(x)$ is computed from the known solution $u(x) = 1 - \sin\left(\frac{5\pi}{4}x\right)$.

4.1.1. Structured nodes

Let us discretize the domain in (13) using N structured nodes and let us use a three nodes $(x - h, x, x + h)$ central difference scheme to approximate the second derivative. The resulting local RBF-FD approximation error is [1]

$$\epsilon_3(x;c) = \frac{h^2}{12}u^{(IV)}(x) + \frac{h^2}{c^2}u''(x) - \frac{3h^2}{4c^4}u(x) + O\left(h^4 P_3(1/c^2)\right). \tag{14}$$

We use the notation $O(h^m P_n(1/c^2))$ to indicate that the terms that have been neglected are of order $h^m \sum_{i=0}^{n}(a_i/c^{2i})$, where a_i are constants which depend on the derivatives and values of the particular function at x. This error is estimated using a finite difference approximation to the exact solution $u(x)$, so $\tilde{u}(x) = u(x) + O(h^2)$. In (14), $u''(x)$ and $u^{(IV)}$ are computed exactly from $f(x)$, so

$$\epsilon_{3e}(x;c) = \frac{h^2}{12}f''(x) + \frac{h^2}{c^2}f(x) - \frac{3h^2}{4c^4}\tilde{u}(x) + O\left(h^4 P_3(1/c^2)\right). \tag{15}$$

and the accuracy of the local error computed with the finite-difference approximation in (15) is of the same order ($O(h^4)$) as the one computed with the exact solution in (14). From now on, we will replace the exact solution $u(x)$ by the finite difference approximation $\tilde{u}$ in all the formulas derived in [1], without loss of precision.

Fig. 1 shows with solid lines the infinity norm of the RBF-FD error, $\|\mathbf{E}(c)\|_\infty = \|\mathbf{u} - \hat{\mathbf{u}}(c)\|_\infty$, as a function of the shape parameter c for different number of nodes N. In all cases, the estimated error given by (15), shown with dot-dashed lines, reproduces closely the RBF-FD error in the limit $c \gg h$. This allows us to estimate c^* accurately using (15). Notice that for

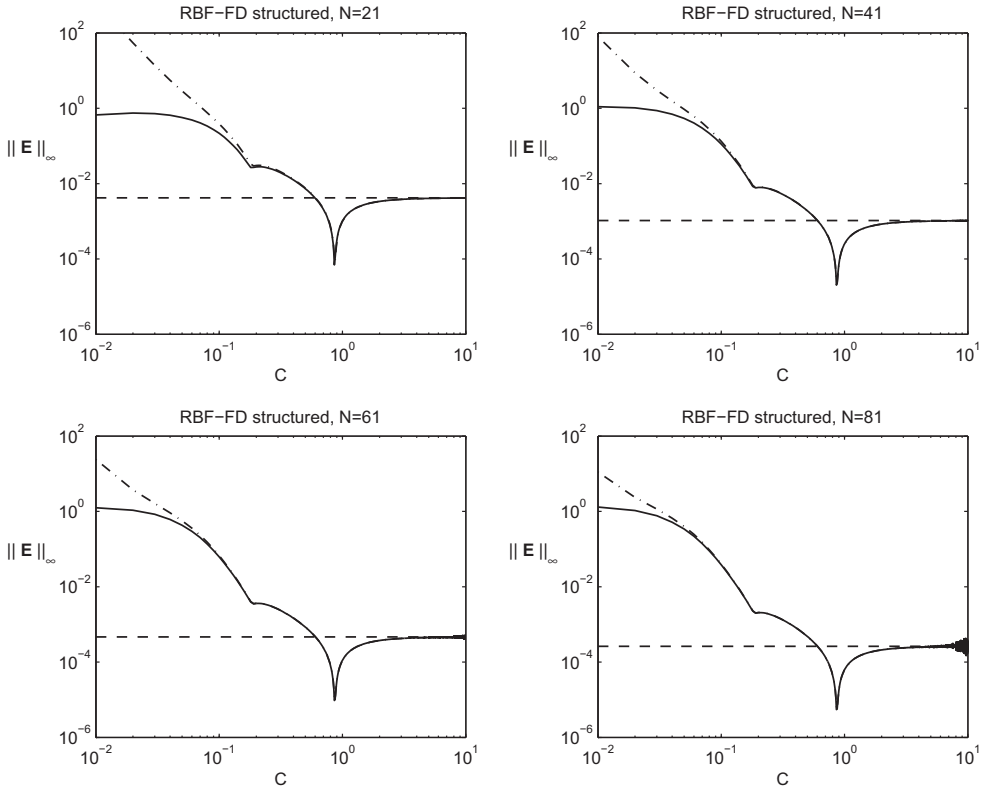

Fig. 1. Infinite norm of the errors of problem (13) as function of c, using $N = 21, 41, 61$, and 81 structured nodes. Solid lines: RBF-FD error (9). Dot-dashed lines: estimated error (15). Dashed lines: finite difference error.

Table 1
Optimal shape parameters and the corresponding errors for problem (13) with structured nodes.

	$N = 21$	$N = 41$	$N = 61$	$N = 81$
$\|\widetilde{\mathbf{E}}\|_\infty$	$4.181 \cdot 10^{-3}$	$1.044 \cdot 10^{-3}$	$4.638 \cdot 10^{-4}$	$2.609 \cdot 10^{-4}$
c^*	0.8589	0.8616	0.8621	0.8623
$\|\mathbf{E}(c^*)\|_\infty$	$6.694 \cdot 10^{-5}$	$1.672 \cdot 10^{-5}$	$7.425 \cdot 10^{-6}$	$4.182 \cdot 10^{-6}$
c_e^*	0.8628	0.8626	0.8625	0.8625
$\|\mathbf{E}(c_e^*)\|_\infty$	$7.763 \cdot 10^{-5}$	$1.735 \cdot 10^{-5}$	$7.541 \cdot 10^{-6}$	$4.216 \cdot 10^{-6}$
$\|c^* - c_e^*\|$	0.0039	0.0010	0.0004	0.0002

large values of c, the RBF-FD error approaches the standard finite-difference error, depicted in Fig. 1 with dashed lines. We observe that there is a range of shape parameters around c^* for which the RBF-FD solution is significantly more accurate than the finite difference solution. Notice also that in the case $N = 81$ ill conditioning appears for large values of c.

From top to bottom, Table 1 shows the infinite norm of the finite difference solution error $\|\widetilde{\mathbf{E}}\|_\infty$, the exact optimal shape parameter c^* and its corresponding error $\|\mathbf{E}(c^*)\|_\infty$, the estimated optimal shape parameter c_e^* and its corresponding error $\|\mathbf{E}(c_e^*)\|_\infty$, and the difference between the exact and the estimated optimal shape parameter. The results are very accurate, since the error in c_e^* is of order $O(h^2)$. Notice that, to leading order, the value of the optimal shape parameter is independent of h (independent of N). Also notice that there is an improvement of approximately two orders of magnitude between the finite difference solution and the optimal RBF-FD solution.

4.1.2. Unstructured nodes

In the case that the domain is discretized with unequally spaced nodes, the local RBF-FD approximation error using a three nodes $(x - h, x, x + \lambda h)$ central difference scheme is

$$\epsilon_3(x;c) = \frac{\lambda-1}{3}hu'''(x) + (\lambda-1)\frac{h}{c^2}u'(x) + [\lambda(\lambda-1)+1]\frac{h^2}{12}u^{(IV)}(x) + \lambda\frac{h^2}{c^2}u''(x) + [\lambda(\lambda-5)+1]\frac{h^2}{4c^4}u(x) + O\left(h^3 P_2(1/c^2)\right). \tag{16}$$

In this case, the local approximation error is only of order $O(h)$ so we also include terms of order $O(h^2)$ in the formula. The resulting approximation to the local error is of order $O(h^3)$ while in the case of structured nodes it was of order $O(h^4)$. To compute the estimated error $\epsilon_{3e}(x;c)$ the derivatives of order greater or equal to two appearing in Eq. (16) are computed exactly from the derivatives of f. The values of u and u' are approximated to first order using finite differences.

Fig. 2 shows the corresponding infinite norm of the error $\|\mathbf{E}(c)\|_\infty$ as function of c for different number of nodes N (we use Halton nodes [20] here). In this case, the error estimation (dot-dashed lines) is as accurate as in the case of structured nodes, but the minimum error corresponding to c_e^* is less pronounced.

Table 2 shows the same information as Table 1 but for unstructured nodes. As before, the optimal shape parameter is estimated accurately $(c^* - c_e^* = O(h^2))$, but the improvements in accuracy with respect to finite differences are less significant (approximately one order of magnitude).

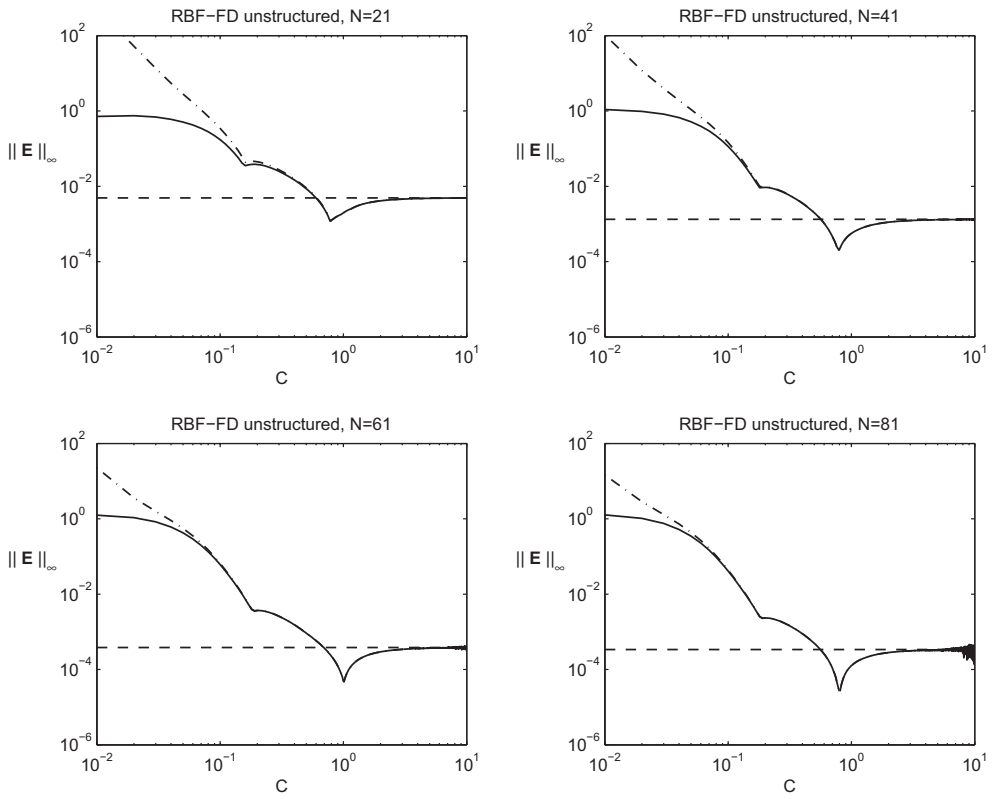

Fig. 2. Same as Fig. 1 but for unstructured nodes.

Table 2
Same as Table 1 but for unstructured nodes.

	$N = 21$	$N = 41$	$N = 61$	$N = 81$
$\|\|\widetilde{\mathbf{E}}\|\|_\infty$	$4.928 \cdot 10^{-3}$	$1.327 \cdot 10^{-3}$	$3.818 \cdot 10^{-4}$	$3.377 \cdot 10^{-4}$
c^*	0.7795	0.7944	1.0063	0.8067
$\|\|\mathbf{E}(c^*)\|\|_\infty$	$1.178 \cdot 10^{-3}$	$1.945 \cdot 10^{-4}$	$4.551 \cdot 10^{-5}$	$2.580 \cdot 10^{-5}$
c_e^*	0.7858	0.7959	1.0069	0.8071
$\|\|\mathbf{E}(c_e^*)\|\|_\infty$	$1.207 \cdot 10^{-3}$	$1.981 \cdot 10^{-4}$	$4.586 \cdot 10^{-5}$	$2.595 \cdot 10^{-5}$
$\|c^* - c_e^*\|$	0.0063	0.0015	0.0006	0.0004

4.2. Steady convection–diffusion problem

Consider the problem

$$\begin{cases} u_x - u_{xx} = \pi^2 \sin(\pi x) + \pi \cos(\pi x), & 0 < x < 1, \\ u(0) = 0, & u(1) = 1 \end{cases} \tag{17}$$

whose exact solution is $u(x) = \sin(\pi x) + \frac{e^x - 1}{e - 1}$. This problem was proposed and solved in [5]. The local approximation error to the convection–diffusion differential operator with the RBF-FD formula using three structured nodes is

$$\epsilon_3(x; c) = \frac{h^2}{12}\left(2u'''(x) - u^{(IV)}(x)\right) + \frac{h^2}{2c^2}\left(u'(x) - 2u''(x)\right) + \frac{3h^2}{4c^4}u(x) + O\left(h^4 P_3(1/c^2)\right). \tag{18}$$

In this formula u is approximated using a second order central difference scheme, and u' is approximated from $\tilde{u}$ using the corresponding second order central difference scheme. Higher derivatives are approximated to second order through the recursion $u^{(k+1)} = \tilde{u}^{(k)} - f^{(k-1)}$ for $k \geqslant 1$.

Fig. 3 shows with solid lines the corresponding infinite norm of the error $\|\mathbf{E}(c)\|_\infty$ as a function of c for different number of nodes N. As in the previous cases, the error estimated with the analytical formulas is in close agreement with the actual error, and therefore, the estimated optimal shape parameter is very accurate.

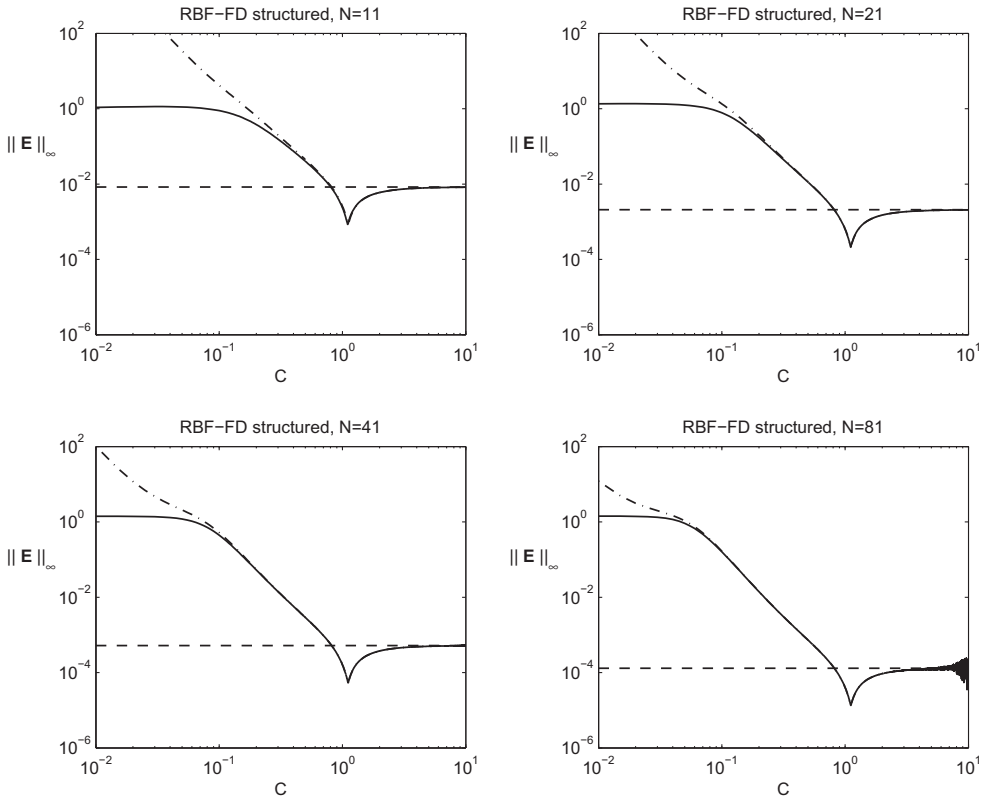

Fig. 3. Infinite norm of the errors of problem (17) as function of c, using $N = 11, 21, 41$, and 81 structured nodes. Solid lines: RBF-FD error (9). Dot-dashed lines: estimated error (18). Dashed lines: finite difference error.

Table 3
Optimal shape parameters and the corresponding errors for problem (17) with structured nodes.

	$N = 11$	$N = 21$	$N = 41$	$N = 81$
$\|\tilde{\mathbf{E}}\|_\infty$	$8.337 \cdot 10^{-3}$	$2.088 \cdot 10^{-3}$	$5.220 \cdot 10^{-4}$	$1.305 \cdot 10^{-4}$
c^*	1.1031	1.1101	1.1116	1.1121
$\|\mathbf{E}(c^*)\|_\infty$	$8.318 \cdot 10^{-4}$	$2.090 \cdot 10^{-4}$	$5.241 \cdot 10^{-5}$	$1.311 \cdot 10^{-5}$
$c^*_{[5]}$	1/0.9	1/0.9	1/0.9	1/0.9
$\|\mathbf{E}(c^*_{[5]})\|_\infty$	$1.43 \cdot 10^{-3}$	$3.83 \cdot 10^{-4}$	$9.75 \cdot 10^{-5}$	$2.45 \cdot 10^{-5}$
c^*_e	1.1139	1.1127	1.1123	1.1123
$\|\mathbf{E}(c^*_e)\|_\infty$	$9.245 \cdot 10^{-4}$	$2.161 \cdot 10^{-4}$	$5.282 \cdot 10^{-5}$	$1.314 \cdot 10^{-5}$
$\|c^* - c^*_e\|$	0.0108	0.0026	0.0007	0.0002

Table 3 shows the same information as Table 1 but for problem (17). As before, the estimated optimal shape parameter is very accurate. In Ref. [5] the optimal shape parameter was computed by trial and error ($c^* = 1/\epsilon^* = 1/0.9 = 1.11$). The authors included a constant term in order to impose the condition that the RBF-FD formulas are exact for constants. The corresponding results were presented in Table IV of [5], and are reproduced here in the fourth and fifth rows of Table 3.

4.2.1. Unstructured nodes

In the case that the domain is discretized with unequally spaced nodes, the local RBF-FD approximation error using a three nodes $(x - h, x, x + \lambda h)$ central difference scheme for the convection–diffusion operator is

$$\epsilon_3(x;c) = \frac{(1-\lambda)}{3} h u'''(x) + (1-\lambda)\frac{h}{c^2}u'(x) + \frac{h^2}{12}\left[2\lambda u'''(x) - [\lambda(\lambda-1)+1]u^{(IV)}(x)\right] + \frac{\lambda h^2}{2c^2}[u'(x) - 2u''(x)] - [\lambda(\lambda-5)+1]\frac{h^2}{4c^4}u(x) + O\left(h^3 P_2(1/c^2)\right). \tag{19}$$

The derivatives appearing in these formulas are approximated in the same way described in the previous section.

As was the case in (16), the local approximation error is only of order $O(h)$ so we include terms of order $O(h^2)$ in this formula too. The resulting approximation to the local error is also of order $O(h^3)$ while in the case of structured nodes it was of order $O(h^4)$.

Fig. 4 shows with solid lines the corresponding infinite norm of the error $\|\mathbf{E}(c)\|_\infty$ as function of c for different number of nodes N (Halton nodes). The error estimation (dot-dashed lines) is as accurate as in the case of structured nodes.

Table 4 summarizes these results. Notice that in this case the optimal shape parameter c^* is more dependent on h. This is due to the fact that the formula for the error is only order h and therefore c^* is independent of h only for large values of N.

4.3. Two dimensional boundary value problem

Consider now the two dimensional Poisson problem

$$\begin{cases} \Delta u = f(x,y), & \text{in } \Omega = (0,1)\times(0,1) \\ u = u(x,y), & \text{on } \partial\Omega \end{cases} \tag{20}$$

where $f(x,y)$ is obtained from the exact solution

$$u = \exp\left[-\left(x-\frac{1}{4}\right)^2 - \left(y-\frac{1}{2}\right)^2\right]\cos(2\pi y)\sin(\pi x). \tag{21}$$

This problem has been used by Wright and Fornberg [43] to test the performance of the local RBF-FD and local RBF-HFD (Hermite RBF) methods.

4.3.1. Structured nodes

Suppose the domain is discretized in $N \times N$ structured nodes. Using a five nodes $\{(x,y),(x-h,y),(x+h,y),(x,y-h),(x,y+h)\}$ central difference scheme, the local RBF-FD error is

$$\epsilon_5(\mathbf{x},c) = \frac{h^2}{12}\left(u^{(4,0)}(\mathbf{x}) + u^{(0,4)}(\mathbf{x})\right) + \frac{5h^2}{6c^2}\left(u^{(2,0)}(\mathbf{x}) + u^{(0,2)}(\mathbf{x})\right) - \frac{7h^2}{6c^4}u(\mathbf{x}) + O\left(h^4 P_3(1/c^2)\right). \tag{22}$$

In this equation u is approximated using second order central differences, $u^{(2,0)} + u^{(0,2)} = f$ is computed exactly, and $u^{(4,0)} + u^{(0,4)} = \Delta f - 2u^{(2,2)}$, where $u^{(2,2)}$ is approximated from $\tilde{u}$ using the corresponding second order central difference scheme.

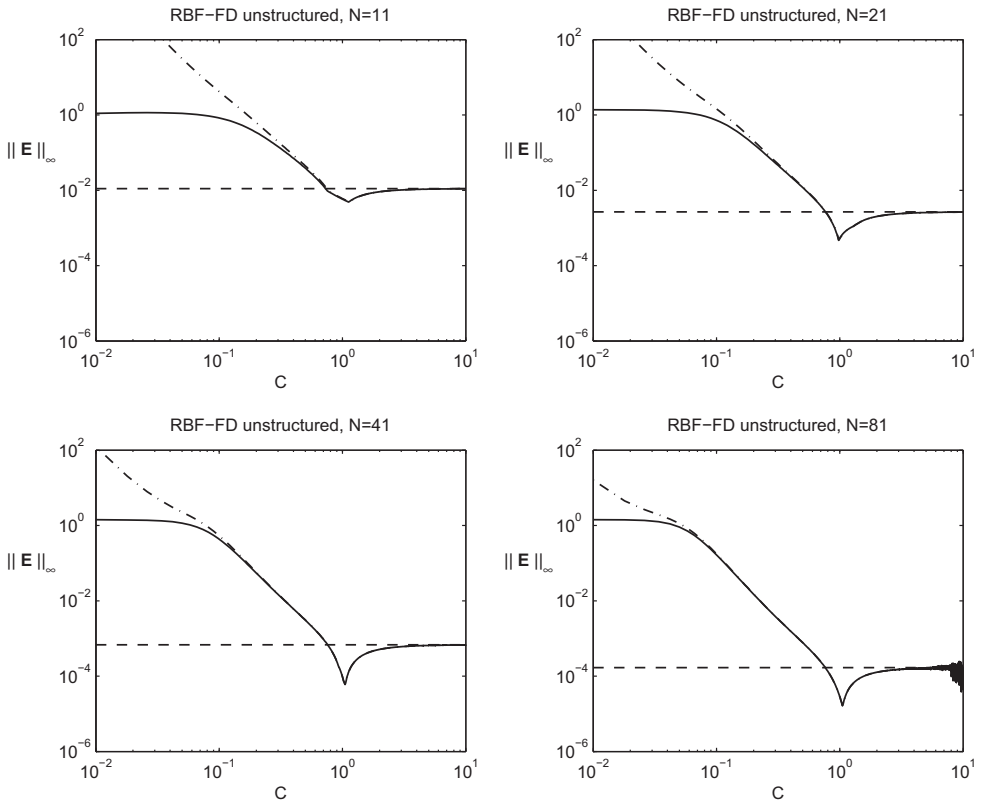

Fig. 4. Same as Fig. 3 but for unstructured nodes.

Table 4
Same as Table 3 but for unstructured nodes.

	$N = 11$	$N = 21$	$N = 41$	$N = 81$
$\|\|\widetilde{\mathbf{E}}\|\|_\infty$	$1.105 \cdot 10^{-2}$	$2.667 \cdot 10^{-3}$	$6.788 \cdot 10^{-4}$	$1.685 \cdot 10^{-4}$
c^*	1.1230	0.9773	1.0525	1.0536
$\|\|\mathbf{E}(c^*)\|\|_\infty$	$4.863 \cdot 10^{-3}$	$4.690 \cdot 10^{-4}$	$5.891 \cdot 10^{-5}$	$1.578 \cdot 10^{-5}$
c_e^*	1.1409	0.9818	1.0536	1.0539
$\|\|\mathbf{E}(c_e^*)\|\|_\infty$	$5.060 \cdot 10^{-3}$	$4.832 \cdot 10^{-4}$	$5.979 \cdot 10^{-5}$	$1.584 \cdot 10^{-5}$
$\|c^* - c_e^*\|$	0.0179	0.0045	0.0011	0.0003

In Fig. 5, we plot with solid lines the infinite norm of the error $\|\mathbf{E}(c)\|_\infty$ as function of c for different number of nodes N. As was the case for the problems in 1D (Figs. 1 and 3) the estimated error using (22), shown with dot-dashed lines, agrees closely with the actual error when $c \gg h$. The agreement improves as N increases (h decreases). For large values of c the RBF-FD error coincides with the standard finite difference error (depicted with dashed lines).

Table 5 shows the same information as the previous tables but for the solution of problem (20). As in previous cases, the estimated optimal shape parameter c_e^* is very close to the exact optimal shape parameter c^*, and there is a very small loss of accuracy resulting from the use of the estimated value c_e^* instead of the exact value c^*. Again, the RBF-FD method is more accurate than the standard finite difference method, although in this case, the difference in accuracy is only of one order of magnitude.

This same problem was solved in Ref. [43]. However, for the local RBF interpolation the authors included a constant term in order to impose the condition that the RBF-FD formulas are exact for constants. Introducing this additional function in the basis used for local interpolation results in the following analytical formula for the local approximation error

$$\epsilon_{5e}(\mathbf{x}, c) = \frac{h^2}{12}\left(\tilde{u}^{(4,0)}(\mathbf{x}) + \tilde{u}^{(0,4)}(\mathbf{x})\right) + + \frac{9h^2}{8c^2}\left(\tilde{u}^{(2,0)}(\mathbf{x}) + \tilde{u}^{(0,2)}(\mathbf{x})\right) + O\left(h^4 P_2(1/c^2)\right). \tag{23}$$

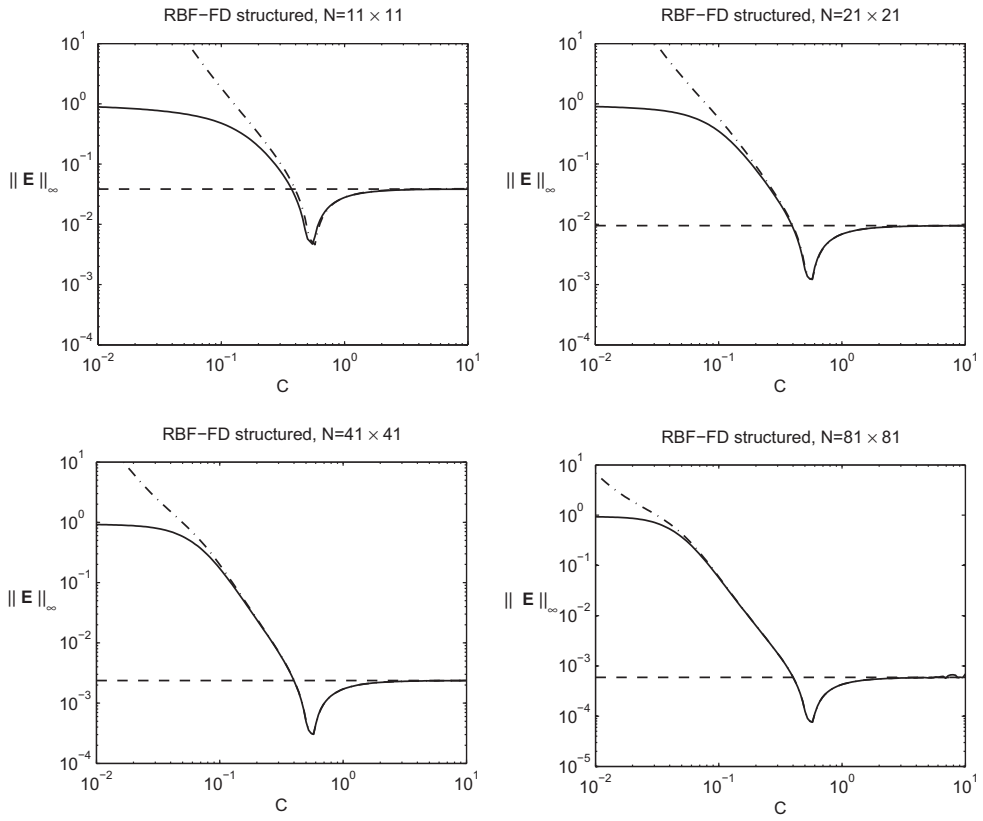

Fig. 5. Infinite norm of the errors of problem (20) with exact solution (21) as function of c, using different number N of structured nodes. Solid lines: RBF-FD error (9). Dot-dashed lines: estimated error (22). Dashed lines: finite difference error.

Table 5
Optimal shape parameters and the corresponding errors for problem (20) with exact solution (21) using structured nodes.

N	11×11	21×21	41×41	81×81
$\|\|\widetilde{\mathbf{E}}\|\|_\infty$	$3.847 \cdot 10^{-2}$	$9.516 \cdot 10^{-3}$	$2.370 \cdot 10^{-3}$	$5.921 \cdot 10^{-4}$
c^*	0.5601	0.5772	0.5807	0.5816
$\|\|\mathbf{E}(c^*)\|\|_\infty$	$4.517 \cdot 10^{-3}$	$1.219 \cdot 10^{-3}$	$3.040 \cdot 10^{-4}$	$7.602 \cdot 10^{-5}$
c_e^*	0.5756	0.5811	0.5816	0.5818
$\|\|\mathbf{E}(c_e^*)\|\|_\infty$	$6.320 \cdot 10^{-3}$	$1.335 \cdot 10^{-3}$	$3.106 \cdot 10^{-4}$	$7.627 \cdot 10^{-5}$
$\|c^* - c_e^*\|$	0.0155	0.0039	0.0009	0.0002

This expression is slightly different from (22). The term proportional to u does not appear. This should be expected since the formula is exact for constant functions. However, this additional degree of freedom has a very small impact on the results as can be appreciated in Fig. 6. In this figure we plot the infinite norm of the errors as function of c ($N = 21 \times 21$) when the RBF-FD solutions are computed with and without the constant term in the interpolation basis (dashed and solid lines, respectively). We also plot the estimated errors for these two cases, with and without the constant term in the interpolation basis (dotted and dot-dashed lines, respectively). We observe that the optimal shape parameter is only slightly modified when the constant term is added to the RBF-FD interpolation.

Table 6 shows the same information as Table 5, but for the case in which a constant term is added to the interpolation. Row 2 shows the results obtained in Ref. [43] (see Table 3 of [43]) for the case $c = 1/1.6 = 0.625$, which gives the most accurate results reported in [43] for the 5 node RBF-FD formula. In this table, we have used the same grids used in [43]. As in previous cases, the analytical approximation to the error makes it possible to accurately compute the optimal shape parameter without knowing the exact solution of the problem.

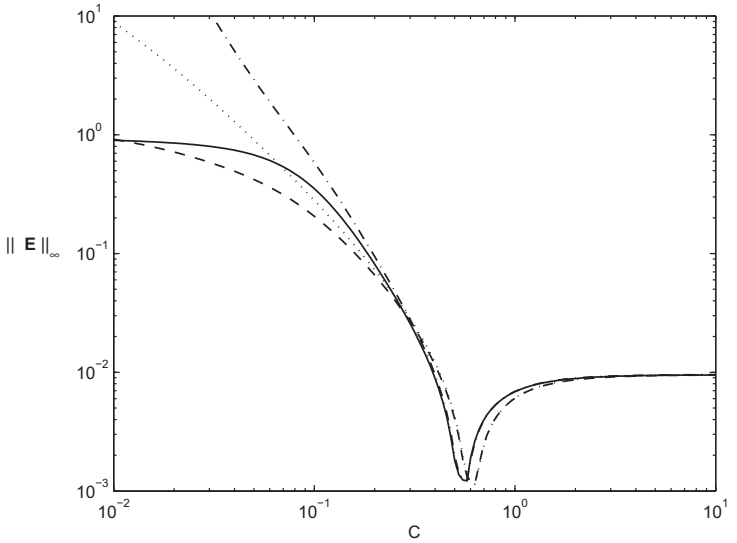

Fig. 6. Infinite norm of the errors of problem (20) with exact solution (21), using $N = 21 \times 21$ structured nodes. Solid line: exact error (9) using local RBF interpolation with no constant term. Dashed line: exact error (9) using local RBF interpolation with constant term. Dot-dashed line: estimated error using (22). Dotted line: estimated error using (24).

Table 6
Same as Table 5 but including a constant term in the RBF interpolation, as in [43].

N	6×6	11×11	21×21	51×51
$\|\widetilde{\mathbf{E}}\|_\infty$	$1.348 \cdot 10^{-1}$	$3.847 \cdot 10^{-2}$	$9.516 \cdot 10^{-3}$	$1.517 \cdot 10^{-3}$
$c_{[43]}$	1/1.6	1/1.6	1/1.6	1/1.6
$\|\mathbf{E}(c_{[43]})\|_\infty$	$2.692 \cdot 10^{-2}$	$4.305 \cdot 10^{-3}$	$1.147 \cdot 10^{-3}$	$1.850 \cdot 10^{-4}$
c^*	0.5899	0.6246	0.6143	0.6445
$\|\mathbf{E}(c^*)\|_\infty$	$1.667 \cdot 10^{-2}$	$4.267 \cdot 10^{-3}$	$1.144 \cdot 10^{-3}$	$1.840 \cdot 10^{-4}$
c_e^*	0.6361	0.6365	0.6176	0.6451
$\|\mathbf{E}(c_e^*)\|_\infty$	$2.993 \cdot 10^{-2}$	$5.457 \cdot 10^{-3}$	$1.145 \cdot 10^{-3}$	$1.857 \cdot 10^{-4}$
$\|c^* - c_e^*\|$	0.0462	0.0119	0.0033	0.0006

4.3.2. Unstructured nodes

Consider now the case in which the domain is discretized using N unstructured nodes. The local RBF-FD error for six unequally spaced nodes $\{(x,y),(x+h,y+\lambda_1 h),(x+\beta_2 h,y+\lambda_2 h),(x+\beta_3 h,y+\lambda_3 h),(x+\beta_4 h,y+\lambda_4 h),(x+\beta_5 h,y+\lambda_5 h)\}$ central difference scheme is [1]

$$\begin{aligned}\epsilon_6(\mathbf{x},c) = {} & h\left[A_{0,0}u^{(3,0)}(\mathbf{x}) + A_{0,1}u^{(2,1)}(\mathbf{x}) + A_{0,2}u^{(1,2)}(\mathbf{x}) + A_{0,3}u^{(0,3)}(\mathbf{x})\right] + \frac{h}{c^2}\left[A_{1,0},u^{(1,0)}(\mathbf{x}) + A_{1,1}u^{(0,1)}(\mathbf{x})\right] \\ & + h^2\left[B_{0,0}u^{(4,0)}(\mathbf{x}) + B_{0,1}u^{(3,1)}(\mathbf{x}) + B_{0,2}u^{(2,2)}(\mathbf{x}) + B_{0,3}u^{(1,3)}(\mathbf{x}) + B_{0,4}u^{(0,4)}(\mathbf{x})\right] \\ & + \frac{h^2}{c^2}\left[B_{1,0},u^{(2,0)}(\mathbf{x}) + B_{1,1}u^{(1,1)}(\mathbf{x}) + B_{1,2}u^{(0,2)}(\mathbf{x})\right] + \frac{h^2}{c^4}B_{2,0}u(\mathbf{x}) + O\left(h^3 P_3(1/c^2)\right),\end{aligned} \tag{24}$$

where the coefficients $A_{i,j}$ and $B_{i,j}$ depend on the surrounding nodes layout $\{\beta_k\}$ and $\{\lambda_k\}$, and its exact values can be computed numerically for each node. In this example, we have not computed numerically the derivatives of $u(\mathbf{x})$ that appear in Eq. (24). Instead, we have used the exact values of the function and its derivatives in order to analyze the convergence of the error and to estimate the optimal shape parameter.

We will use an unstructured node layout of N^2 nodes: $N^2 - 4(N-1)$ Halton nodes [20] in the interior of the domain and $4(N-1)$ structured nodes on the boundary (see Fig. 7). For the local support, we will use stencils with $n = 6$ nodes. For standard finite differences, 6 nodes stencils allow, in principle, a consistent approximation to the Laplacian operator (i.e. the approximation is at least first order accurate) since there are six constraints that have to be satisfied. However, there are special configurations of the nodes in the stencil for which there is no solution to the constraints [34], and therefore the coefficients of the finite difference formula cannot be computed. The problem of stencil support selection for unstructured nodes is a very crucial topic in finite differences which has been addressed by several authors. In a recent paper, Davydov and Oanh

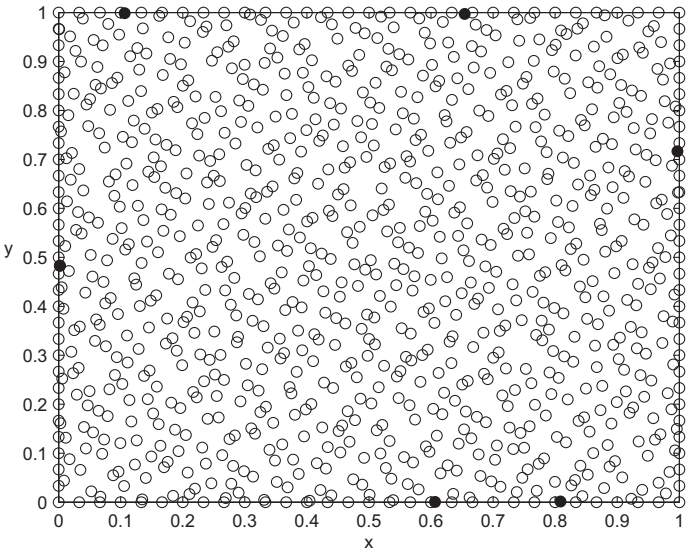

Fig. 7. Unstructured node layout with 961 nodes: 841 Halton nodes inside the domain and 120 structured nodes on the boundary. Filled circles are the nodes removed from the set after applying Seibold's algorithm.

[7] reviewed different support selection methods and proposed a new algorithm based on minimizing the sum of the squares of the angles between two consecutive lines from the central node to the other nodes in the stencil.

We also have found that (at least with Halton nodes) arbitrary stencils using nearest nodes sometimes leads to an ill-conditioned system for large values of c. Therefore, we apply a modified version of the algorithm recently proposed by Seibold [35] to select a valid six node stencil. The algorithm is based on a linear programming approach that guarantees the positivity of the stencil. Since the coefficients of RBF-FD for a given stencil coincide with the coefficients of FD in the limit $c \to \infty$, and since Seibold's algorithm guarantees the positivity of scattered FD stencils, then it also guarantees the positivity of the RBF-FD stencil in that limit. In fact, we have found this to be the case in all the experiments that we have done. Applying Seibold's algorithm to the Halton nodes shown in Fig. 7, results in a 6 node stencil selection for almost all the interior nodes. There are a few nodes, usually very close to the boundary, for which Seibold's algorithm does not yield a solution. Those nodes are removed from the set (these are shown as filled circles in Fig. 7), and Seibold's algorithm is applied again until a valid finite difference 6 node stencil is assigned to each node. Then, steps 2–4 of the numerical algorithm described in Section 3 are applied in order to compute the optimal RBF-FD solution. Starting from valid finite difference stencils insures the validity of the corresponding RBF-FD stencils.

Plots of the RBF-FD and estimated errors for different number of nodes N appear in Fig. 8 with solid and dot-dashed lines, respectively. We observe again an excellent agreement between them. We tabulated the main results in Table 7, in which we show the number of nodes in the grid and in parenthesis the number of nodes remaining after applying Seibold's algorithm. The error achieved with the estimated optimal shape parameter $\|\mathbf{E}(c_e^*)\|_\infty$ is very close to the optimal one $\|\mathbf{E}(c^*)\|_\infty$ in all the cases. As expected, the difference between the exact optimal parameter c^* and the estimated one c_e^* decreases with the number of nodes N.

4.3.3. Additional Poisson equation examples

In this section, we address the solution of several problems defined by the Poisson equation which have been proposed in the past. In all cases, we consider Eq. (20) with the function f computed, in each case, from the following exact solutions:

$$u_1 = \sin(\pi x)\sin(\pi y), \tag{25}$$

$$u_2 = \frac{\arctan\left[2(x+3y-1)\right]}{\arctan\left[2(\sqrt{10}+1)\right]}, \tag{26}$$

$$u_3 = 0.75\exp\left[-\frac{(9x-2)^2+(9y-2)^2)}{4}\right] + 0.75\exp\left[-\frac{(9x+1)^2}{49}-\frac{9y+1}{10}\right] + 0.5\exp\left[-\frac{(9x-7)^2+(9y-3)^2}{4}\right] - 0.2\exp\left[-(9x-4)^2-(9x-7)^2\right], \tag{27}$$

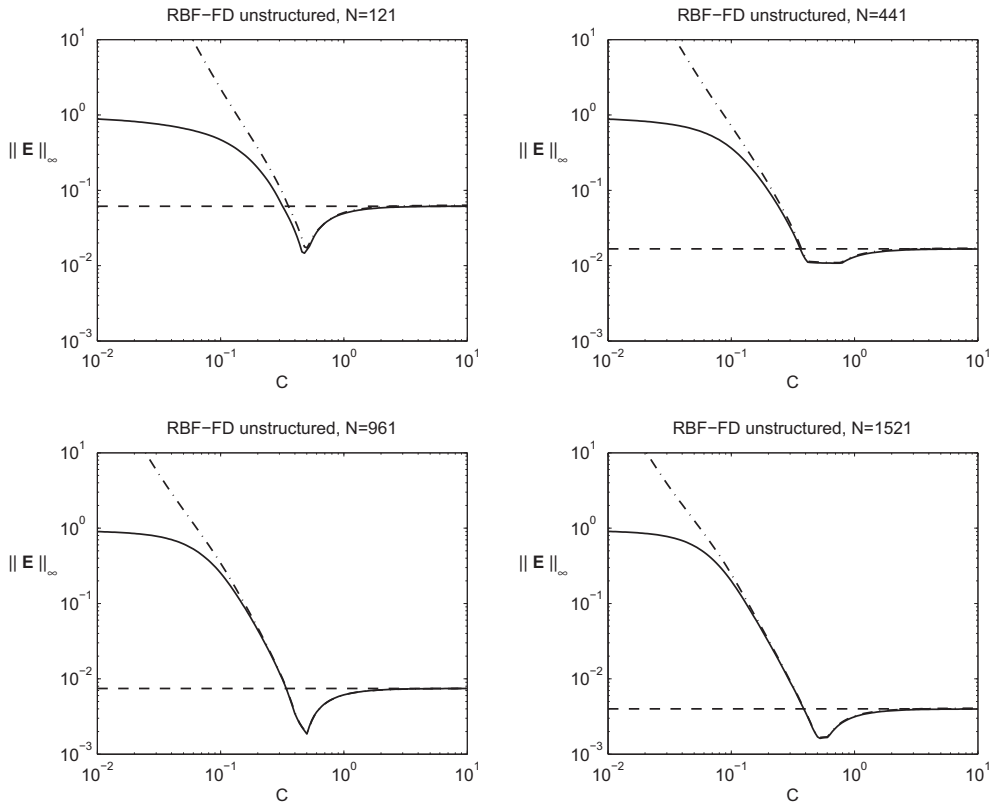

Fig. 8. Same as Fig. 5 but for unstructured nodes.

Table 7
Same as Table 5 but for unstructured nodes.

N	121 (120)	441 (438)	961 (955)	1521 (1513)
$\|\|\widetilde{\mathbf{E}}\|\|_\infty$	$6.153 \cdot 10^{-2}$	$1.668 \cdot 10^{-2}$	$7.454 \cdot 10^{-3}$	$3.983 \cdot 10^{-3}$
c^*	0.4655	0.7871	0.5027	0.5113
$\|\|\mathbf{E}(c^*)\|\|_\infty$	$1.360 \cdot 10^{-2}$	$1.079 \cdot 10^{-2}$	$1.841 \cdot 10^{-3}$	$1.616 \cdot 10^{-3}$
c_e^*	0.4869	0.7783	0.5058	0.5094
$\|\|\mathbf{E}(c_e^*)\|\|_\infty$	$1.519 \cdot 10^{-2}$	$1.079 \cdot 10^{-2}$	$1.911 \cdot 10^{-3}$	$1.630 \cdot 10^{-3}$
$\|c^* - c_e^*\|$	0.0214	0.0088	0.0031	0.0019

$$u_4 = \frac{25}{25 + (x - 0.2)^2 + 2y^2}. \tag{28}$$

Fig. 9 shows with solid lines the infinite norm of the error $\|\mathbf{E}(c)\|_\infty$ as a function of c for the four problems considered here (problems (25)–(28)). In these problems, we have used a regular mesh of 31×31 nodes. Notice that in all cases the estimated errors computed with Eq. (22), shown with dot-dashed lines, are in close agreement with the RBF-FD errors for $c \gg h$, and that there is always a range of shape parameters for which the RBF-FD solution is more accurate than the standard FD solution (the FD error is shown in dashed lines).

Table 8 compares the results obtained with finite differences, and with RBF-FD using the optimal shape parameter computed either from the exact solution or from Eq. (22).

Problem (25) was first proposed by Ding et al. [8] to numerically analyze the dependence of the approximation error with shape parameter c, local density of nodes h, and number of supporting nodes n. They used equally spaced nodes in their numerical experiments and concluded that for $n \leqslant 9$ the error behaves as $\|\mathbf{E}\| \approx O((h/c)^{1.9})$. Our analysis in [1] shows that the error behaves as $\|\mathbf{E}\| \approx O((h/c)^2)$ (see, for instance, Eq. (22)). Problem (25) has also been used by Davydov and Oanh [7]. In Fig. 7 of their paper the root mean square (rms) error of the numerical differentiation error and the solution error are displayed as a function of c. They use a value of the shape parameter as large as possible with the RBF matrix still numerically non-singular. Thus, they operate the RBF-FD method in the region where it is equivalent to finite differences, and this is

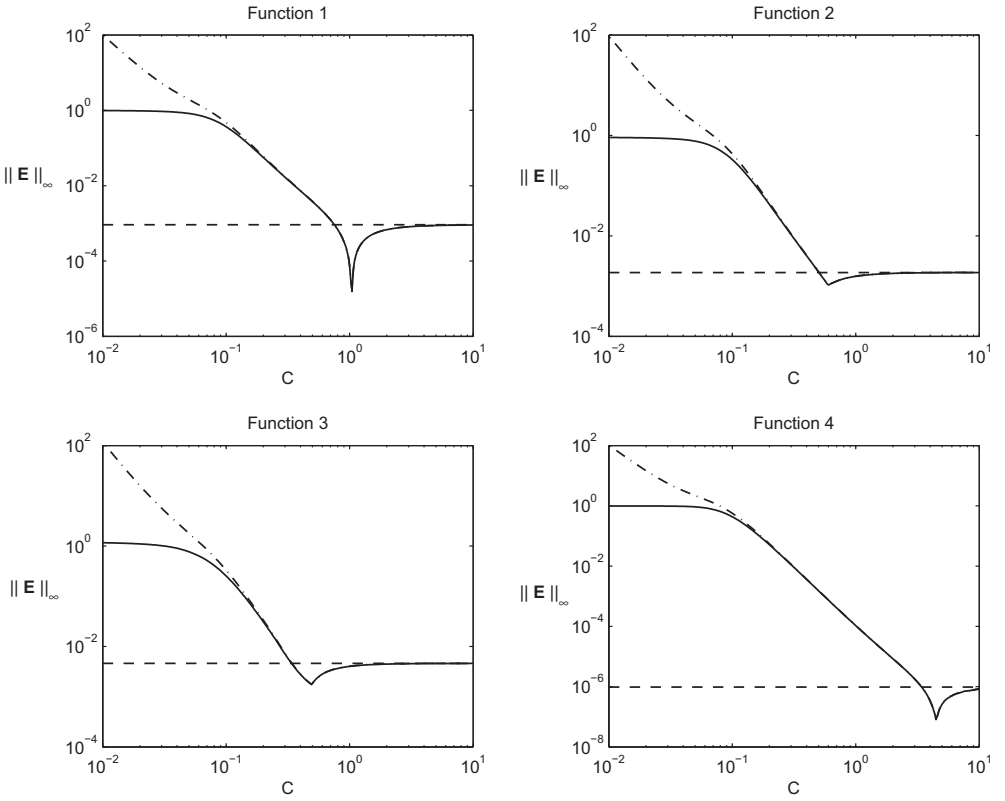

Fig. 9. Infinite norm of the errors of problem (20) with exact solutions (25)–(28), using $N = 31 \times 31$ structured nodes.

Table 8
Optimal shape parameters and the corresponding errors for problem (20) with exact solutions (25)–(28), using a 31×31 structured grid.

	u_1	u_2	u_3	u_4
$\|\widetilde{\mathbf{E}}\|_\infty$	$9.144 \cdot 10^{-4}$	$1.868 \cdot 10^{-3}$	$4.604 \cdot 10^{-3}$	$9.727 \cdot 10^{-7}$
c^*	1.0380	0.5978	0.4922	4.4949
$\|\mathbf{E}(c^*)\|_\infty$	$7.092 \cdot 10^{-8}$	$1.043 \cdot 10^{-3}$	$1.742 \cdot 10^{-3}$	$7.436 \cdot 10^{-8}$
c_e^*	1.0387	0.5978	0.4935	4.4957
$\|\mathbf{E}(c_e^*)\|_\infty$	$1.345 \cdot 10^{-6}$	$1.043 \cdot 10^{-3}$	$1.758 \cdot 10^{-3}$	$7.440 \cdot 10^{-8}$
$\|c^* - c_e^*\|$	0.0007	0.0000	0.0013	0.0008

confirmed in Fig. 7 of their paper, where the RBF-FD errors are undistinguishable from those of finite differences. From that figure, and for $N = 31 \times 31$ ($1/N = 10^{-3}$), the rms of the numerical differentiation error is approximately $9 \cdot 10^{-3}$ and the rms of the solution error is approximately $4 \cdot 10^{-4}$. Using the optimal shape parameter c_e^*, we obtain an rms for the numerical differentiation error of $4.7 \cdot 10^{-7}$, and an rms for the solution error of $2.4 \cdot 10^{-8}$. The reason for this extremely high accuracy is that, for this problem, it is straightforward to verify that the shape parameter that minimizes the local approximation error (22) is independent of location. Thus, the optimal (constant) shape parameter c_e^* that we use in our computations minimizes the error at every point of the grid.

Problem (26) was used by Larsson and Fornberg [27] to analyze the global RBF method for infinitely smooth basis functions ($c \to \infty$). The problem was solved in the unit disk using 50 unstructured nodes. Of the six problems considered in [27], problem (26) was the most hard to solve ($\|\mathbf{E}\|_\infty = 0.23$ for the optimal shape parameter $c^* = 1/0.89 = 1.124$). The results in Fig. 9 and Table 8 show that, also with the local RBF method, the errors are relatively high. In addition, it can be observed that, with a constant shape parameter, there is very little accuracy increase with respect to finite differences. This can be due to the fact that, either there are many locations for which there is not a local optimal shape parameter, or the optimal local shape parameter varies much with location and there is not a single (constant) optimal shape parameter c^* which can be successfully used at all locations.

Problem (27) was also proposed by Ding et al. [8]. The solution is quite hilly, having three relative extrema and one saddle point within the domain. As in the previous problem, the solution error and the optimal shape parameter are accurately computed with Eq. (22), but there is little improvement with respect to finite differences.

Problem (28) was solved in [27,43] on the unit disk using unstructured nodes and 9 node stencils. The minimum value of the infinite norm of the solution error with an unstructured set of 200 nodes (shown in Fig. 4 of [43]) is approximately $1.6 \cdot 10^{-5}$. The results in Table 8 show that, for a regular rectangular mesh of 961 nodes and 5 node stencils, the infinite norm of the error is $7.440 \cdot 10^{-8}$. The reason for this high accuracy is that function (28) is almost constant throughout the domain and, therefore, using a single (constant) optimal shape parameter for all the nodes results in highly accurate solutions. In fact, in Ref. [1] the optimal shape parameter that minimizes the local approximation error for a nine node stencil at location (0,0) was $c = 1/0.2617 = 3.82$ and this result varies very little with location.

5. Conclusions

In this paper we describe how to predict the solution error using the RBF-FD method with a single (constant) value of the shape parameter. It is based on analytical formulas derived in [1] for the local approximation error of RBF-FD formulas. Since the error can be accurately predicted, it is also possible to accurately estimate the optimal shape parameter that minimizes the solution error.

We have described the technique through several examples in 1D (3 node stencils) and 2D (5 and 6 node stencils) using both structured and unstructured nodes. However, the formulas derived in [1] can also be used to solve problems with other stencils. We emphasize that to compute the optimal shape parameter to order $O(h^2)$ it is only necessary to approximate the solution $u(\mathbf{x})$ and certain derivatives to order $O(h^2)$. In practice, this can be achieved by first computing the standard finite difference solution, then use this solution to estimate the optimal shape parameter c_e^*, and finally use this value to compute the optimal RBF-FD solution. For unstructured grids in 2D it is not advisable to estimate derivatives through finite difference formulas, since this will require the selection of appropriate stencils for each derivative. Instead, one can use the RBF global method on a coarse grid and use this solution to approximate $u(\mathbf{x})$ and the needed derivatives on the unstructured grid.

From the point of view of computational cost the technique requires solving the problem twice; first with standard finite differences and then with the RBF-FD method. Thus, for the solution of a Poisson problem in 2D using N nodes, the method requires the solution of two sparse linear systems of $N \times N$ unknowns. However, it is possible to take advantage of the fact that, to leading order, the optimal shape parameter is independent of h. Thus, the finite difference solution or the global RBF solution needed to estimate c_e^*, can be computed in a coarse grid, and then the RBF-FD method can be used to compute the final solution in a fine grid. In this way the computational cost can be significantly reduced.

Acknowledgements

This work has been supported by Spanish MICINN grants FIS2010-18473, CSD2010-00011 and by Madrid Autonomous Region grant S2009-1597.

References

[1] V. Bayona, M. Moscoso, M. Carretero, M. Kindelan, RBF-FD formulas and convergence properties, J. Comput. Phys. 229 (2010) 8281–8295.
[2] V. Bayona, M. Moscoso, M. Kindelan, Optimal (variable) shape parameter for multiquadric based RBF-FD method, J. Comput. Phys. (submitted for publication).
[3] F. Bernal, M. Kindelan, Use of singularity capturing functions in the solution of problems with discontinuous boundary conditions, Eng. Anal. Boundary Elem. 33 (2009) 200–208.
[4] R.E. Carlson, T.A. Foley, The parameter R2 in multiquadric interpolation, Comput. Math. Appl. 21 (1991) 29–42.
[5] G. Chandhini, Y.V.S.S. Sanyasiraju, Local RBF-FD solutions for steady convection–diffusion problems, Int. J. Numer. Methods Eng. 72 (2007) 352–378.
[6] S. Chantasiriwan, Investigation of the use of radial basis functions in local collocation method for solving diffusion problems, Int. Commun. Heat Mass Transfer 31 (2004) 1095–1104.
[7] O. Davydov, D.T. Oanh, Adaptive meshless centers and RBF stencils for Poisson equation, J. Comput. Phys. 230 (2011) 287–304.
[8] H. Ding, C. Shu, D.B. Tang, Error estimates of local multiquadric-based differential quadrature (LMQDQ) method through numerical experiments, Int. J. Numer. Methods Eng. 63 (2005) 1513–1529.
[9] T.A. Driscoll, B. Fornberg, Interpolation in the limit of increasingly flat radial basis functions, Comput. Math. Appl. 43 (2002) 413–422.
[10] T.A. Driscoll, A.R.H. Heryudono, Adaptive residual subsampling methods for radial basis function interpolation and collocation problems, Comput. Math. Appl. 53 (2007) 927–939.
[11] G.E. Fasshauer, Meshfree Approximation Methods with MATLAB, World Scientific Publishing Co., Singapore, 2007.
[12] G.E. Fasshauer, J.G. Zhang, On choosing "optimal" shape parameters for RBF approximation, Numer. Algor. 45 (2007) 345–368.
[13] A.J.M. Ferreira, C.M.C. Roque, G.E. Fasshauer, R.M.N. Jorge, R.C. Batra, Analysis of functionally graded plates by a robust meshless method, Mech. Adv. Mater. Struct. 14 (2007) 577–587.
[14] A.J.M. Ferreira, G.E. Fasshauer, R.C. Batra, J. Dias Rodrigues, Analysis of natural frequencies of composite plates by an RBF-pseudospectral method, Compos. Struct. 79 (2007) 202–210.
[15] N. Flyer, E. Lehto, Rotational transport on a sphere: local node refinement with radial basis functions, J. Comput. Phys. 229 (2010) 1954–1969.
[16] B. Fornberg, G.B. Wright, Stable computation of multiquadric interpolants for all values of the shape parameter, Comput. Math. Appl. 48 (2004) 853–867.
[17] B. Fornberg, J. Zuev, The Runge phenomenon and spatially variable shape parameters in RBF interpolation, Comput. Math. Appl. 54 (2007) 379–398.
[18] B. Fornberg, E. Letho, Stabilization of RBF-generated finite difference methods for convective PDEs, J. Comput. Phys. 230 (2011) 2270–2285.
[19] R. Franke, Scattered data interpolation: tests of some method, Math. Comput. 38 (1982) 181–200.
[20] J. Halton, On the efficiency of certain quasi-random sequences of points in evaluating multi-dimensional integrals, Numer. Math. 2 (1960) 84–90.

[21] R.L. Hardy, Multiquadric equations of topography and other irregular surfaces, J. Geophys. Res. 176 (1971) 1905–1915.
[22] C.-S. Huang, C.-F. Lee, A.H.-D. Cheng, Error estimate, optimal shape factor, and high precision computation of multiquadric collocation method, Eng. Anal. Boundary Elem. 31 (2007) 614–623.
[23] E.J. Kansa, Multiquadrics, a scattered data approximation scheme with applications to computational fluid dynamics. I. Surface approximations and partial derivatives estimates, Comput. Math. Appl. 19 (1990) 127–145.
[24] E.J. Kansa, Multiquadrics, a scattered data approximation scheme with applications to computational fluid dynamics. II. Solutions to parabolic, hyperbolic and elliptic partial differential equations, Comput. Math. Appl. 19 (1990) 147–161.
[25] E.J. Kansa, R.E. Carlson, Improved accuracy of multiquadric interpolation using variable shape parameters, Comput. Math. Appl. 24 (1992) 99–120.
[26] E.J. Kansa, Y.C. Hon, Circumventing the ill-conditioning problem with multiquadric radial basis functions: applications to elliptic partial differential equations, Comput. Math. Appl. 39 (2000) 123–137.
[27] E. Larsson, B. Fornberg, A numerical study of some radial basis function based solution methods for elliptic PDEs, Comput. Math. Appl. 46 (2003) 891–902.
[28] E. Larsson, B. Fornberg, Theoretical and computational aspects of multivariate interpolation with increasingly flat radial basis functions, Comput. Math. Appl. 49 (2005) 103–130.
[29] C. Lee, X. Liu, S. Fan, Local multiquadric approximation for solving boundary value problems, Comp. Mech. 30 (2003) 396–409.
[30] S. Rippa, An algorithm for selecting a good value for the parameter c in radial basis function interpolation, Adv. Comput. Math. 11 (1999) 193–210.
[31] C.M.C. Roque, D. Cunha, C. Shu, A.J.M. Ferreira, A local radial basis functions-finite differences technique for the analysis of composite plates, Eng. Anal. Boundary Elem. 35 (2011) 363–374.
[32] Y.V.S.S. Sanyasiraju, G. Chandhini, Local radial basis function based gridfree scheme for unsteady incompressible viscous flows, J. Comput. Phys. 227 (2008) 8922–8948.
[33] B. Sarler, R. Vertnik, Meshfree explicit local radial basis function collocation method for diffusion problems, Comput. Math. Appl. 51 (2006) 1260–1282.
[34] B. Seibold, M-matrices in meshless finite difference methods, PhD thesis, Department of Mathematics, University of Kaiserslautern, Shaker-Verlag, 2006.
[35] B. Seibold, Minimal positive stencils in meshfree finite difference methods, Comput. Methods Appl. Mech. Eng. 198 (2008) 592–601.
[36] Y.Y. Shan, C. Shu, N. Qin, Multiquadric Finite Difference (MQ-FD) method and its application, Adv. Appl. Math. Mech. 1 (2009) 615–638.
[37] C. Shu, H. Ding, K.S. Yeo, Local radial basis function-based differential quadrature method and its application to solve two-dimensional incompressible Navier–Stokes equations, Comput. Methods Appl. Mech. Eng. 192 (2003) 941–954.
[38] D. Stevens, H. Power, M. Leesa, H. Morvan, The use of PDE centres in the local RBF Hermitian method for 3D convective–diffusion problems, J. Comput. Phys. 228 (2009) 4606–4624.
[39] A.I. Tolstykh, D.A. Shirobokov, On using radial basis functions in a "finite difference mode" with applications to elasticity problems, Comput. Mech. 33 (2003) 68–79.
[40] J.G. Wang, G.R. Liu, A point interpolation meshless method based on radial basis functions, Int. J. Numer. Meth. Eng. 54 (2002) 1623–1648.
[41] J. Wertz, E.J. Kansa, L. Ling, The role of the multiquadric shape parameters in solving elliptic partial differential equations, Comput. Math. Appl. 51 (2006) 1335–1348.
[42] G.B. Wright, Radial basis function interpolation: numerical and analytical developments, Ph.D. thesis, University of Colorado, Boulder, 2003.
[43] G.B. Wright, B. Fornberg, Scattered node compact finite difference-type formulas generated from radial basis functions, J. Comput. Phys. 212 (2006) 99–123.